

The laser-induced electron-hole liquid in the diamond: critical lattice temperature and non-equilibrium carrier density

Evgeniy I. Lipatov*^a, Dmitrii E. Genin^a, Denis V. Grigor'ev^{a,b}, Victor F. Tarasenko^{a,b}

^aInstitute of High Current Electronics SB RAS, 2/3 Akademicheskoy Avenue, Tomsk, Russian Federation, 634055

^bTomsk State University, 36 Lenin Avenue, Tomsk, Russian Federation, 634050

ABSTRACT

Integrated photoluminescence spectra of two diamond samples under laser radiation excitation at 193 and 222 nm, depending on the temperature in the range of 80-300 K and the peak intensity in the range of 7-13 MW/cm², were investigated. At temperatures below 200 K, and the peak intensity of more than 10 MW/cm² of laser radiation at 222 nm, the radiative recombination band of electron-hole liquid was observed in integrated photoluminescence spectra of CVD diamond sample.

Keywords: Diamond, exciton, electron-hole liquid, electron-hole pair, luminescence, ultraviolet, laser

1. INTRODUCTION

Electron-hole liquid (EHL) in diamond is observed at much higher temperatures than in other semiconductors^{1,2}. The exact value of the EHL formation critical temperature in diamond is still subject to debate, but it is at least $T_{crit} > 138$ K¹. While other semiconductors critical temperature takes values less than 100 K³. The critical concentration in a diamond formation EHL $n_{crit} \sim 10^{19}$ cm⁻³ is also significantly higher than (one to three orders of magnitude) one in other semiconductors³. So, the EHL in diamond exists in totally different conditions, which create additional difficulties for its observation. On the other hand the study of EHL in diamond enables to refine the theory of the electron-hole liquid formation in semiconductors.

Investigations of EHL in diamond are carried out using laser generation of electron-hole pairs (EHP). EHL is usually excited by sub-picosecond laser pulses, since the relaxation of electronic excitations in undoped diamond occur in the time scale of hundreds of picoseconds - tens of nanoseconds^{4,5}. The peak intensity of the laser radiation usually has the value 1-100 GW/cm². Nanosecond laser pulses provide quasi-stationary EHL excitation since the processes of photogeneration and thermalization of EHP, the formation of free excitons (FE) and EHL condensation have subnanosecond time scale. A moderate density of excitation in the few to tens of MW/cm² is usually used.

In our work, we managed to observe the electron-hole liquid radiative recombination band in the integrated spectra of photoluminescence (PL) of the diamond sample synthesized by the chemical vapor deposition (CVD) method excited by laser radiation at 222 nm with a peak intensity of 10-13 MW/cm².

1.1 Electron-hole liquid in semiconductors

In 1968 academician LV Keldysh predicted the existence of the EHL in semiconductors⁶. EHL is a condensed state of the electron-hole plasma, which occurs at low temperatures and high concentrations of electron-hole pairs (EHP). At low temperatures the EHP form a hydrogen-atom-like quasiparticles - free excitons (FE). At low FE concentrations in the semiconductor they can be considered as an ideal gas, consisting of virtually interacting particles. When the FE concentration is increased they form the exciton complexes (EC) due to the Coulomb interaction - trions (ehh and eeh) and biexcitons which act as condensation nuclei of EHL drops. This EHL is not a molecular fluid, as carriers are free to migrate through the drop, which is typical for liquid metal (e.g., liquid alkali metals).

*lipatov@loi.hcei.tsc.ru; phone +7 3822 492-392; fax +7 3822 492-410; www.hcei.tsc.ru

EHL was experimentally found in many semiconductors in the form of droplets surrounded by an exciton gas. EHL was observed in semiconductors that have indirect energy gap structure (Ge, Si, SiC and C) and the direct-gap structure (GaAs, CdS, CdTe, etc.). Two methods to obtain the necessary concentration of the EHP are usually used: injection of carriers through the contacts, photoexcitation of optical photons with energies higher than the band gap of the material or the excitation by electron beams.

Table 1. Characteristics of some indirect-band semiconductors associated with the formation of the EHL: the dielectric constant, the binding energy of an exciton, the exciton radius, the critical temperature and concentration for the formation of an EHL.

Semiconductor	Dielectric constant, ϵ	Binding energy of free exciton, E_x [meV]	Radius of free exciton, a_x [nm]	Critical EHL carrier density, n_{crit} [cm ⁻³]	Critical temperature, T_{crit} [K]
Germanium, Ge	15.6	3.2	15.37	$8.9 \cdot 10^{16}$	6.7
Silicon, Si	11.4	14.3	4.15	$1.2 \cdot 10^{18}$	28
Silicon carbide, 3C-SiC	9.7	13.5	3	$2.3 \cdot 10^{18}$	41
Gallium phosphide, GaP	9.1	10	5	$2.6 \cdot 10^{18}$	45
Diamond, C	5.7	80.5	1.26	$3 \cdot 10^{19}$	165

EHL has a low specific density 10^{-7} - 10^{-8} kg/m³, high charge carrier mobility (moving speed approaches the sonic speed in the crystal) and according to work³ should have metallic type of conductivity. Unlike conventional fluids lifetime of EHL has typical values of nano- to microseconds due to the finite lifetime of the EHP. EHL is observed in the spectra of photo-, cathode- or electroluminescence. Related phenomena to observe the EHL is radiative recombination of FE. The marker of EHL formation is a broad structureless band shifted to longwave range from a relatively narrow recombination band of FE^{2,3}. Under certain conditions, the EC radiative recombination band can be observed between the bands of EHL and FE.

In indirect-band semiconductors conditions for observing the EHL are the most favorable since these semiconductors has multi-valley band structure, thus EHP plasma is degenerate, which facilitates the phase liquid-gas transition^{2,3}.

Fig.1 shows the experimental and calculated values of the critical temperature and concentration of EHP for FE gas - EHL transition in various semiconductors, taken from the literature². The power-law dependence characterizing the relationship between the critical temperature T_{crit} and the critical concentration n_{crit} for the EHL condensation, for various semiconductors is similar to the expression⁷:

$$T_{crit} = Const \cdot \frac{n_{crit}^{\frac{1}{3}}}{\epsilon}, \quad (1)$$

where ϵ is the dielectric constant of the semiconductor. Pay attention to the scatter of values in Fig.1 for conventional semiconductors (Ge and Si).

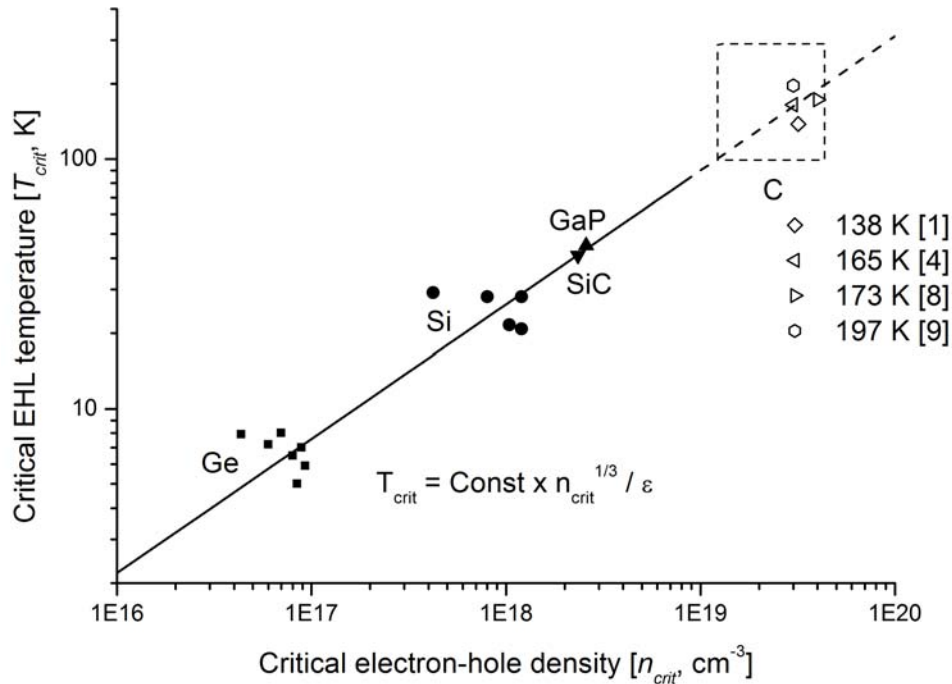


Figure 1. Dependence of the critical temperature of the existence of the electron-hole liquid T_{crit} on the critical concentration of electron-hole pairs n_{crit} in a variety of semiconductors. The data for germanium and silicon are drawn from the review²; for SiC and GaP – from⁷. For the diamond the values from the literature^{1,4,8,9} are shown. The range of possible values T_{crit} and n_{crit} for diamond is limited by a dotted line.

1.2 Electron-hole liquid in diamond

The phase transition EHP plasma - EHL occurs when the EHP concentration is above and the critical temperature is below the critical point for the sample. For germanium concentration n_{crit} and temperature T_{crit} of the phase transition is $8.9 \cdot 10^{16} \text{ cm}^{-3}$ and 6.7 K respectively. For silicon - $1.2 \cdot 10^{18} \text{ cm}^{-3}$ and 28 K, respectively. The typical size of the EHL drops in Ge and Si is 10-100 microns. Under the uniaxial compression of germanium sample a drop of up to 1 mm in diameter was observed³.

The third simple semiconductor with indirect-multi-valley structure of the conduction band is diamond. It's indirect band gap of 5.49 eV, the dielectric constant is 5.7. Calculations showed that the EHL in diamond should be formed with an EHP concentration (in EHL drops) of 10^{20} cm^{-3} and a temperature below 138 K¹.

Natural diamond is heavily contaminated with nitrogen impurity which forms the variety of defects, including polyatomic, containing vacancies, interstitial sites, and other impurity atoms¹⁰. In addition, diamond is a metastable form of carbon (in normal conditions, it is energetically favorable for carbon to crystallize as graphite). Therefore, in the face-centered diamond lattice formed by sp^3 -hybridized covalent bonds, their own structural defects are inevitably built with sp^2 -hybridized bonds. Such defects are the centers of radiative and non-radiative recombination of electron-hole plasma¹¹. At the same time, such defects as a substitute boron and nitrogen atoms at concentrations of up to 10^{18} cm^{-3} can act as centers of EHL droplets condensation¹².

Taken before¹ attempts to find the EHL in natural diamond did not lead to the desired result.

The first success was achieved by Teofilov, Zaitsev and others in 2000, using nanosecond photoexcitation (wavelength 219 nm) of synthetic diamond grown under high pressure and high temperature (HPHT), which was isotopically pure

(¹³C isotope content of less than 0.1%) and nominally undoped¹³. Diamond sample was cooled to a temperature $T = 120$ K. EHL was observed as a broad band in the PL spectrum with a maximum at 239 nm (see Fig.2, curve 1).

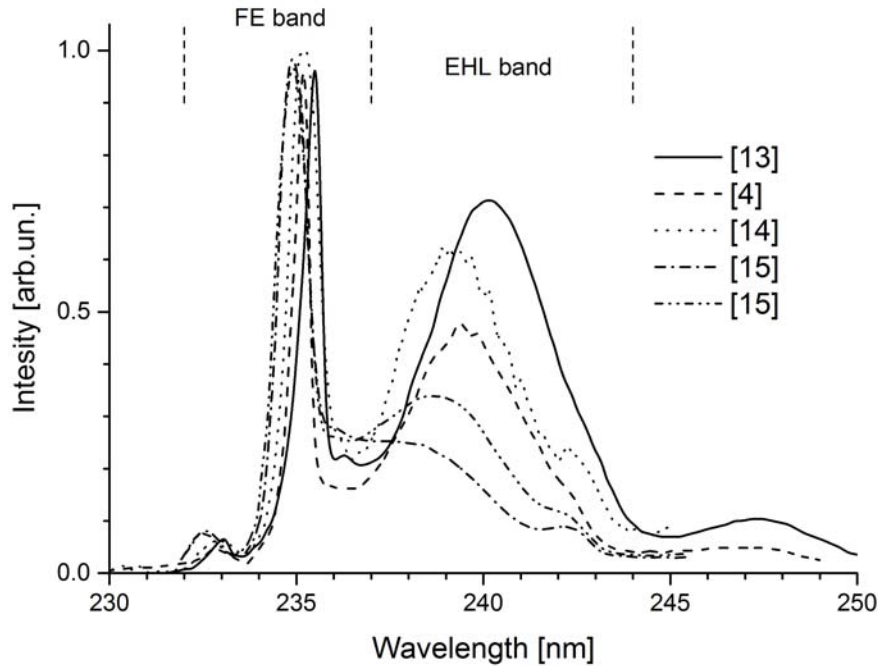


Figure 2. Time-integrated photoluminescence spectra of diamond samples from literature^{4,13-15} with recombination bands of free excitons and electron-hole liquid. [13] - HPHT-diamond, FL excitation wavelength $\lambda = 219$ nm, pulse duration $\tau_{219} = 5$ ns, pulse energy $E_{219} = 520$ μ J, intensity on the sample $I_{219} =$ no data, sample temperature $T = 123$ K; [4] - HPHT, $\lambda = 202$ nm, $\tau_{202} = 200$ fs, $E_{202} = 0.2$ μ J, $I_{202} = 25600$ MW/cm², $T = 15$ K; [14] - CVD, $\lambda = 220$ nm, $\tau_{220} = 5$ ns, $E_{220} =$ no data, $I_{220} =$ no data, $T = 30$ K; [15]-1 - CVD, $\lambda = 200$ nm, $\tau_{200} = 80$ fs, $E_{200} = 0.02$ μ J, $I_{200} = 6400$ MW/cm², $T = 13$ K; [15]-2 - CVD, $\lambda = 200$ nm, $\tau_{200} = 80$ fs, $E_{200} = 0.08$ μ J, $I_{200} = 25700$ MW/cm², $T = 13$ K.

Two years later, Shimano, Nagai et al., using femtosecond laser pulses with a wavelength of 202 nm and HPHT diamond of unknown impurities observed EHL composition at temperatures below $T = 165$ K⁴ (see. Fig.2, Curve 2). Measurement of the photoluminescence spectra with high temporal resolution showed that the EHL is formed with a delay of 50-60 ps after the beginning of the excitation pulse.

In 2009, Donato, Messina et al. observed the radiative recombination of electron-hole liquid in the synthetic CVD diamond cooled to $T = 30-80$ K¹⁴ (see. Fig.2, curve 3). The sample had a thickness of 0.11 mm, and according to the Raman spectra was characterized as high-quality sample. Photoexcitation was provided by laser radiation with a wavelength of 220 nm and pulse duration of 5 ns FWHM.

Note that in^{13,14} it is impossible to define, what value of the peak intensity of the laser radiation was used to excite the EHL.

In¹⁵ CVD diamond cooled to a temperature of 13 K, excited by laser radiation at 200 nm with a pulse width 80 fs and the peak intensity of 300 MW/cm² an appearing of the long-wave shoulder of the FE radiative recombination band was shown. This long-wave shoulder transformed into EHL radiative recombination band with increasing of the peak radiation intensity. The maximum of the EHL band shifted from 238 to 240 nm (see Fig.2, curves 4 and 5).

In¹⁵ it was noted that the main factor limiting the lifetime of the EHL is the Auger recombination of charge carriers because of their high concentration in the EHL ($> 10^{20}$ cm⁻³).

In⁹ we investigated the PL of CVD polycrystalline diamond under cooling with liquid nitrogen ($T \geq 80$ K) and laser excitation at 222 nm with pulse duration of 8 ns FWHM. The long-wave shoulder in PL-spectra appeared since the laser radiation intensity became more than 3 MW/cm². The spectral resolution of the registration system was about 1.5 nm.

2. EXPERIMENTAL

Object of research are the two mono-crystal diamonds that had dimensions $5 \times 5 \times 0.25 \text{ mm}^3$. Sample C10 was synthesized by CVD-method, the sample C12 - by HPHT-method. The absorption spectrum of the sample C10 is shown in Fig.3. Samples were Iia type and had a low content of impurities and defects (nitrogen concentration less than $5 \cdot 10^{17} \text{ cm}^{-3}$). The samples were visually clear, with no visible inclusions.

For PL excitation of the samples we used a pulsed laser radiation at $\lambda = 193 \text{ nm}$ and 222 nm (universal electric-discharge laser "Photon-2", a mixture of $\text{F}_2 / \text{He} / \text{Ar} / \text{Ne} = 3 \text{ Torr} / 57 \text{ Torr} / 60 \text{ Torr} / 3 \text{ atm}$ and a mixture of $\text{HCl} / \text{Kr} / \text{Ne} = 3 \text{ torr} / 120 \text{ torr} / 3 \text{ atm}$) with a pulse energy of up to $E = 30 \text{ mJ}$, pulse duration 8 ns (FWHM) and pulse repetition frequency 1 Hz . Fig.3 shows the emission spectrum of the laser for KrCl-mixture, measured with a monochromator MDR-12 and photocathode FEC-22SPU according to the procedure described in¹⁶. Due to the high absorption coefficient of the diamond in the fundamental absorption range ($\alpha_{193} > 5000 \text{ cm}^{-1}$ and $\alpha_{222} > 350 \text{ cm}^{-1}$) the transparency of the diamond sample was less than 10^{-6} at wavelengths of laser radiation. Therefore diamond samples played the role of optic filters that protect optical devices that detect photoluminescence glow from the laser light which intensity on the surface of diamond sample reached $I_{193} = 6 \text{ MW/cm}^2$ and $I_{222} = 13 \text{ mW/cm}^2$. The energy of the laser radiation was measured with a calorimeter OPHIR with sensor head PE-50BB.

The sample was placed in a vacuum chamber and cooled by liquid nitrogen. The laser beam was focused by a cylindrical quartz lens 2 with focal length 65 mm . Passing through the quartz window pulsed laser radiation excited photoluminescence of the sample inside the vacuum chamber. Lens focus was located within the chamber at a distance of 10 mm from the sample. This rectangular laser beam at the output mirror of the laser beam was converted to a square one on the sample surface.

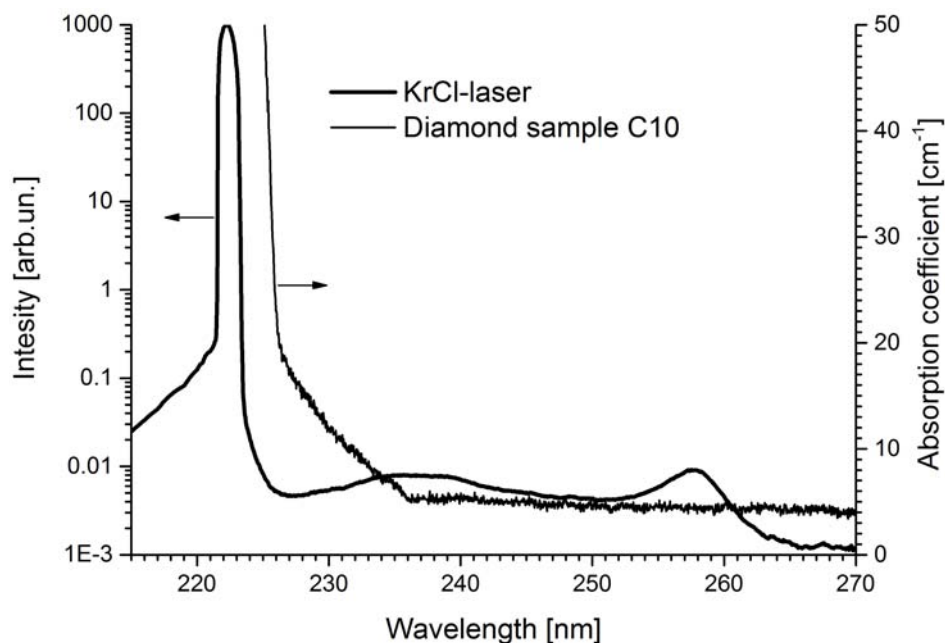


Figure 3. The emission spectrum KrCl-laser (thick) and absorption spectrum of the diamond sample C10 at room temperature (thin). In the spectrum of the KrCl-laser dominated band at $\lambda = 222 \text{ nm}$ is due to laser gain transition $B \rightarrow X$ of KrCl^* molecule. Other bands observed are due to spontaneous emission discharge plasma: the band with a maximum at $\lambda = 258 \text{ nm}$ - $D' \rightarrow A'$ transitions in molecules Cl_2^* , a continuum in the spectral range $\lambda = 225\text{-}250 \text{ nm}$ - transition $C \rightarrow A$ molecules KrCl^* . The absorption spectrum of the diamond sample was observed at the edge of the fundamental absorption $\lambda < 226 \text{ nm}$; the absorption of the diamond in the range $\lambda = 226\text{-}236 \text{ nm}$ is due to optical transitions to the excitonic states.

The sample was mounted on a cooled copper holder using thermal paste KPT-8. The hollow copper heat sink was cooled by the liquid nitrogen. Thus, the sample was cooled from room temperature (RT) to the minimum temperature $T_{\min} = 80 \text{ K}$. The sample temperature was controlled by platinum thermistor (Heraeus Pt 1000 C420), which resistance was

measured by Mustech MY63. The temperature of the sample 4 was calculated from the temperature dependence of the resistance of the thermistor.

The glow of the PL, excited in the layer of the sample with the thickness $\Delta d \sim 50$ microns, passed through the sample and then through the optical fiber to the spectrometer Ocean Optics HR 4000, equipped with a diffraction grating and a CCD line. The spectral resolution of the spectrometer was 0.4 nm.

In the experiments, the vacuum chamber was continuously pumped out by the forevacuum pump until a residual pressure of $p \sim 10^{-1}$ Torr, which allowed, firstly, to avoid water condensation on the sample, and secondly, to decrease the heat exchange between the cooled items and chamber walls by means of air (in the absence of pumping the temperature did not fall below $T = 100$ K).

A more detailed structure of the vacuum chamber and the measurement procedure given in⁹.

3. RESULTS AND DISCUSSION

For the sample C10 in the range of experimental temperatures for an excitation wavelength of 193 and 222 nm with an intensity of from 6 to 13 MW/cm², the radiative recombination band of free excitons with transverse optical phonons FE_{TO} at 235.2 nm dominated in the integrated photoluminescence spectra (see Fig.1a, b). In addition, the two-phonon component (with Raman phonon) FE_{TO+O}^Γ was observed at 242.3 nm. At low temperatures in integrated photoluminescence spectra we manage to observe a component of the radiative recombination of free excitons with transverse acoustic phonons FE_{TA} at 232.7 nm. The increasing of the temperature lead to a significant broadening of the dominant FE_{TO} component. In general, the temperature dependence of the radiative recombination of free excitons was similar^{14,17}.

In the low-temperature photoluminescence when the sample C10 was excited by 222 nm laser radiation at intensities of more than 10 MW/cm² we saw a long-wavelength shoulder (see. Fig.4b and Fig.5a), while with the 193 nm excitation is shoulder was lower (see. Fig.4a), despite the much bigger density of excitation ($n_{193} = 1.4 \cdot 10^{20}$ cm⁻³ \gg $n_{222} = 2.8 - 3.7 \cdot 10^{19}$ cm⁻³). The spectral position and temperature behavior of the shoulder points to its connection with the radiative recombination of electron-hole liquid with transverse optical phonons EHL_{TO} with a spectral peak at 239.8 nm¹².

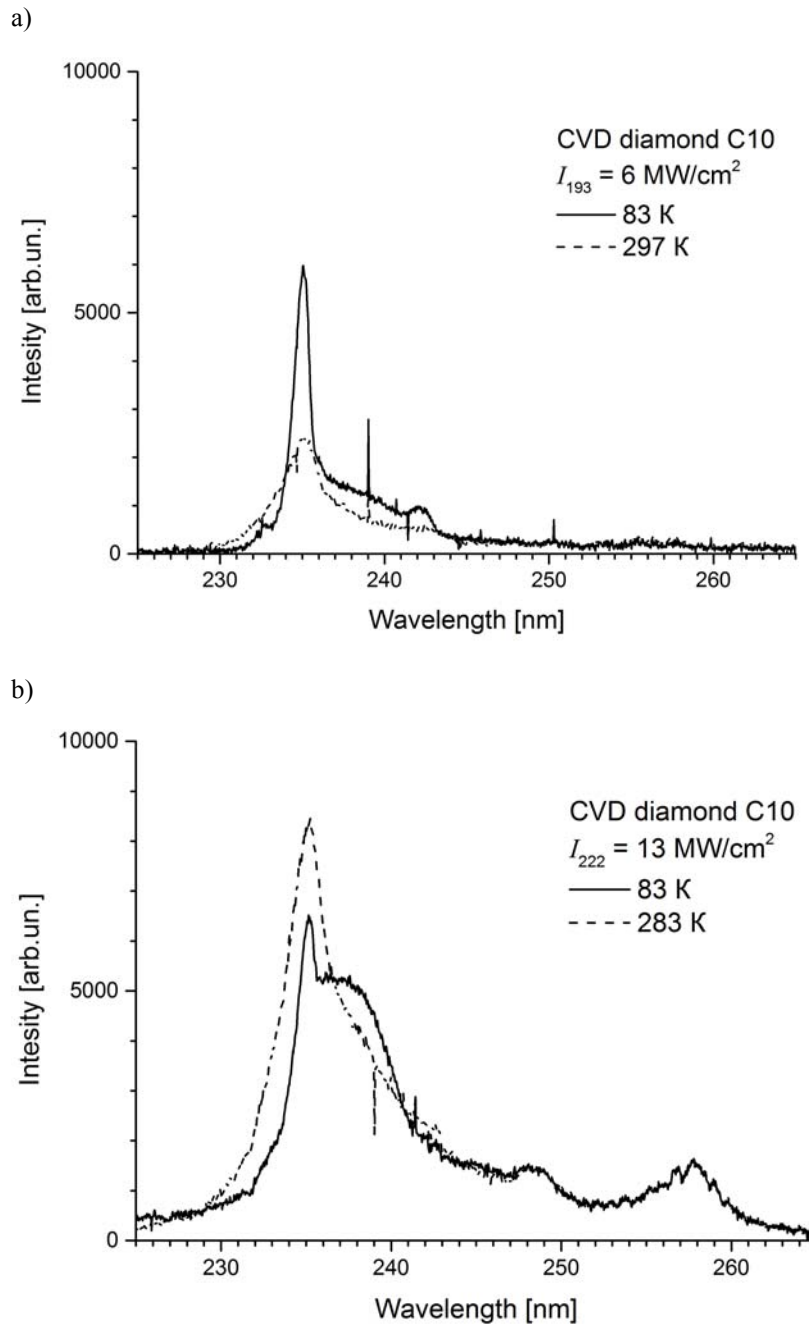


Figure 4. Integrated PL spectra CVD diamond sample C10 excited by lasers at $\lambda = 193$ nm (a) and $\lambda = 222$ nm (b) under cooling with liquid nitrogen and room temperature. When excited photoluminescence at $\lambda = 193$ nm laser intensity was $I_{193} = 6 \text{ MW/cm}^2$, which corresponds to the maximum concentration of electron-hole pairs near the surface of the sample $n_{193} = 1.4 \cdot 10^{20} \text{ cm}^{-3}$. When excited photoluminescence at $\lambda = 222$ nm laser intensity was $I_{222} = 13 \text{ MW/cm}^2$, which corresponds to the maximum concentration of electron-hole pairs near the surface of the sample $n_{222} = 3.7 \cdot 10^{19} \text{ cm}^{-3}$.

Fig.5a, b shows the integral PL spectra of the sample C10 as a function of the peak intensity of the laser radiation. At the temperature $T = 81\text{ K}$ (Fig.5a inset) the increasing of intensity from 7 to 13 MW/cm^2 causes a slight increasing (by a power law with exponent 0.13) of the intensity of the FE_{TO} band at 235.2 nm . At RT similar increase in intensity resulted in the growth of the FE_{TO} band by a power law with an exponent of 1.38 (Fig.5b inset).

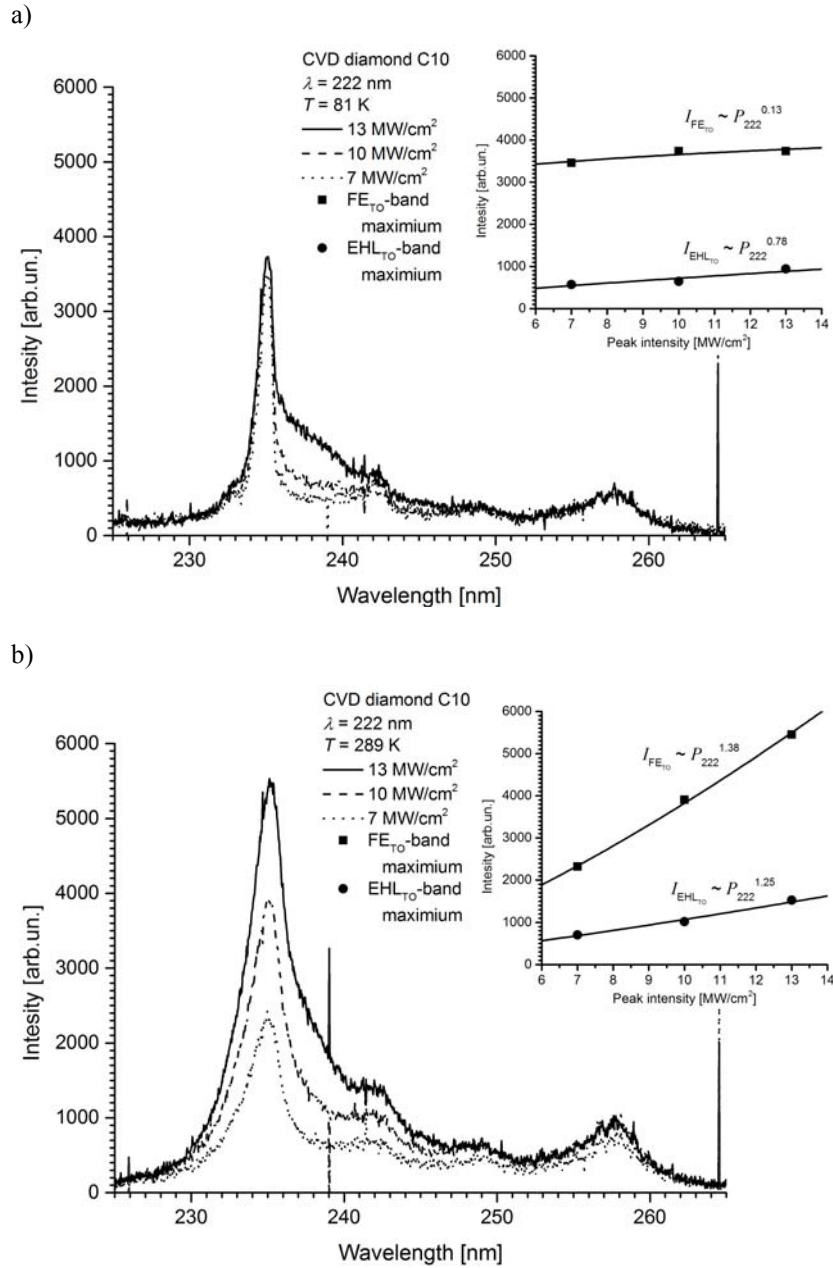


Figure 5. Integrated PL spectra CVD diamond sample C10 with laser excitation at $\lambda = 222\text{ nm}$ under cooling with liquid nitrogen (a) and RT (b). At laser intensities $I_{222} = 7, 10$ and 13 MW/cm^2 the maximum concentration of electron-hole pairs near the surface of the sample were $1.7 \cdot 10^{19}, 2.8 \cdot 10^{19}$ and $3.7 \cdot 10^{19}\text{ cm}^{-3}$, respectively. Insets: dependencies of PL intensity at wavelengths of 235.2 and 239.8 nm (FE_{TO} and EHL_{TO} , respectively) on the peak intensity of the laser radiation.

PL intensity at a wavelength of 239.8 nm (EHL band) with cooling by liquid nitrogen grew by a power law with an exponent of 0.78 with increasing of the excitation density (Fig.5a inset). However, at the RT the slope increased to 1.25 (Fig.5b inset). In the latter case, the increase in the PL intensity at a wavelength of 239.8 nm is not due to increase in intensity of the EHL_{TO} band, but due to the thermal broadening of FE band, because the sample temperature was substantially higher than the critical temperature of condensation in diamond EHL 138-193 K^{1,4,8,9} (see. Fig.1).

For HPHT sample C12 cooled with liquid nitrogen radiative recombination EHL_{TO} band at 239.8 nm is clearly not observed (see. Fig.6). You can note the presence of radiation in the spectral range of 237-240 nm, but it may be glow of the discharge plasma of KrCl-laser (see. Fig.3). If the observation of EHL is possible in the PL spectra of the sample C12, it will occur at higher excitation densities. At the same time, dependences of PL intensities of sample C12 at wavelengths of 235.2 and 239.8 nm (FE_{TO} and EHL_{TO}, respectively) on the peak intensity of the laser radiation (see. Fig.6 inset) were fundamentally different from those for a sample of C10 (see. insert Fig.5a, b).

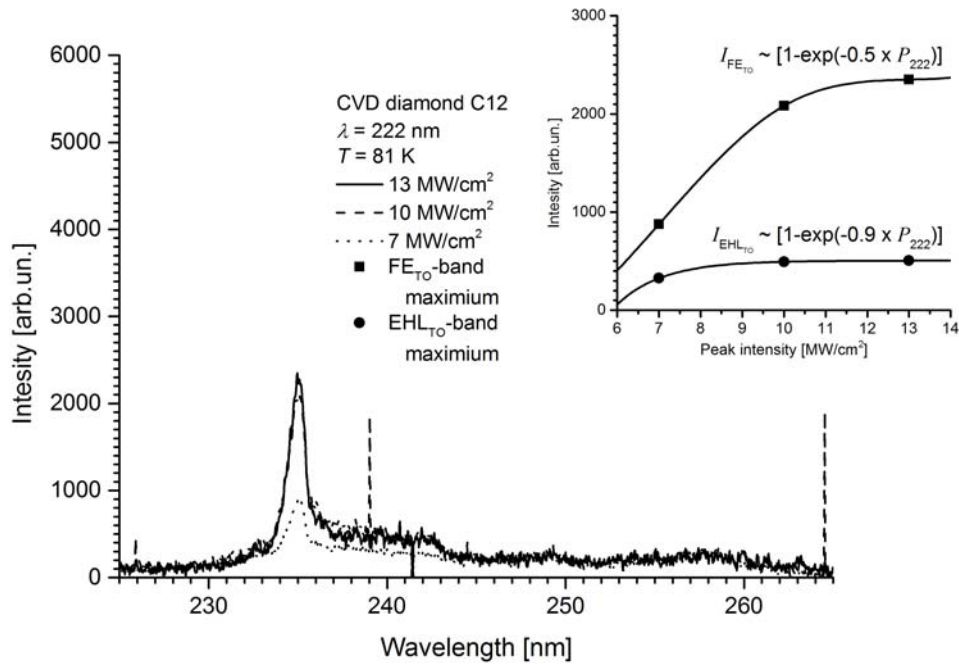


Figure 6. Integrated PL spectra CVD diamond sample C12 excited by laser radiation at $\lambda = 222$ nm when cooled with liquid nitrogen at room temperature. At laser intensities $I_{222} = 7, 10$ and 13 MW/cm² the maximum concentration of electron-hole pairs near the surface of the sample were $1.7 \cdot 10^{19}, 2.8 \cdot 10^{19}$ and $3.7 \cdot 10^{19}$ cm⁻³, respectively. Inset: dependencies of PL intensity at wavelengths of 235.2 and 239.8 nm (FE_{TO} and EHL_{TO}, respectively) on the peak intensity of the laser radiation.

In^{14,17} at low excitation intensities less 1 MW/cm² (i.e. in the absence of FE condensation effects) authors showed that the intensity of the radiative recombination is associated with the FE lifetime. This temperature dependence of the FE band intensity has extreme character with a maximum at 150 K. The strong excitation in¹² with a concentration above the critical FE changes this temperature dependence. It's maximum moves to the high-temperature range due to the increasing of excitation density, because in the temperature range of the EHL existence (at temperatures less than critical) the FE lifetime decreases because of FE condensing into EHL drops.

In Fig.7 shows the temperature dependence of the FE_{TO} band intensity at different peak radiation intensity at 222 nm (7, 10 and 13 MW / cm²) for samples of C10 (Fig.7a) and C12 (Fig.7b).

In the integrated PL spectra of the sample C10, the EHL radiative recombination band was observed (see. Fig.4b and Fig.5a). Temperature dependencies of FE_{TO} band intensity showed the temperature shift of the maximum from 150 K (in the absence of condensation EHL) to 200-210 K with the laser intensity, providing condensation EHL (Fig.7a). This observation is consistent with experimental data¹².

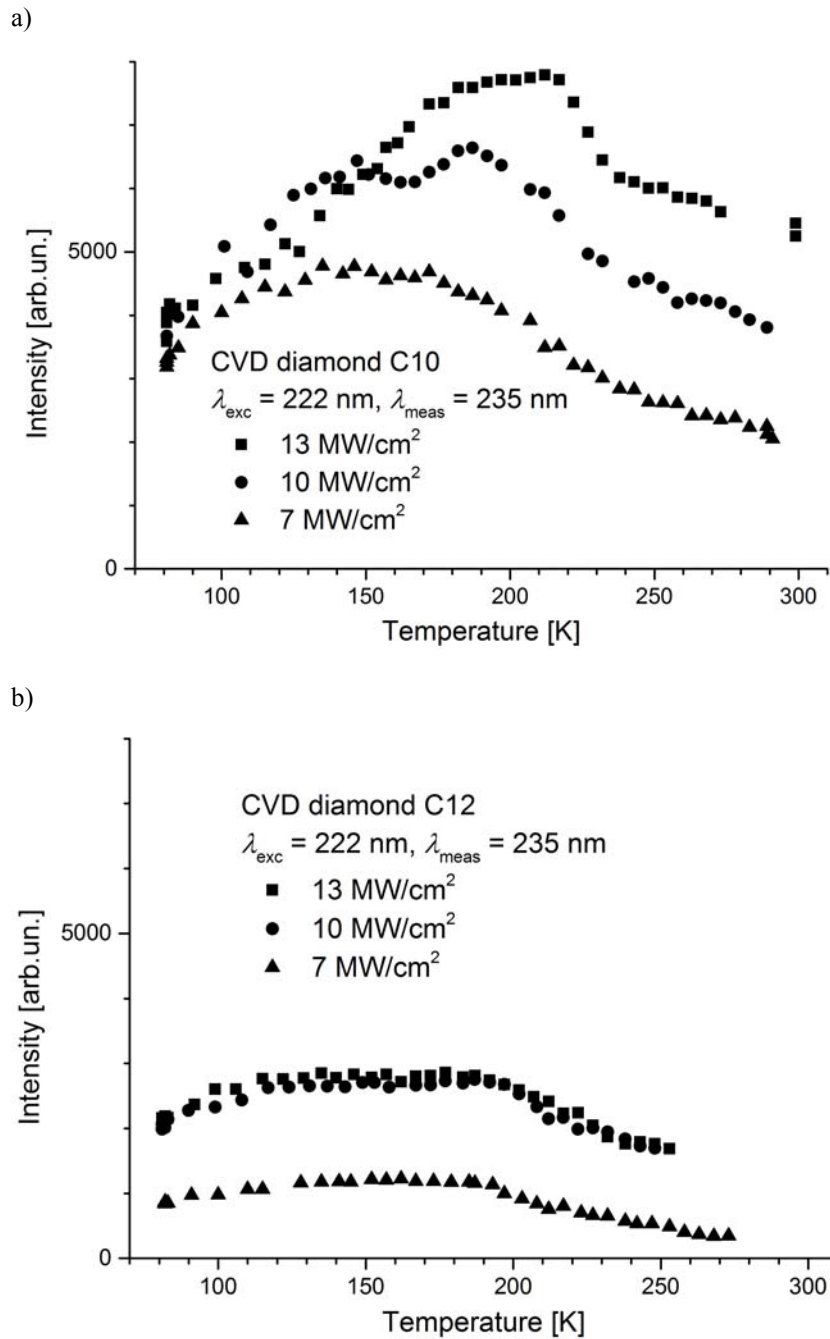


Figure 7. Temperature dependence of the intensity of the radiative recombination FE_{TO} band at laser intensities $I_{222} = 7, 10$ and 13 MW/cm^2 sample C10 (a) and 12C (b).

For sample C12 radiative recombination EHL band was not observed (see. Fig.6) and the temperature dependence of the FE_{TO} band intensity did not change with the increase of the peak intensity of the laser radiation and show a maximum at 150 K (see. Fig.7b), similar with results of works^{12,17}.

4. PHASE DIAGRAM, CRITICAL LATTICE TEMPERATURE AND NON-EQUILIBRIUM CARRIER DENSITY

Making of the phase diagram of the electron-hole system in diamond as a function of temperature on the concentration of charge carriers is important and partly unsolved problem. In^{5,8,18} using the experimental data and theoretical models it were reported results of making the phase diagram that shown on Fig.8.

In^{8,18} experimental data (white squares on Fig.8) were approximated in the model of a degenerate plasma with the critical values of temperature $T_{crit} = 173$ K and the concentration $n_{crit} = 4.05 \cdot 10^{19} \text{ cm}^{-3}$ (curve 1-1 on Fig.8), and in the model of simple liquid near the critical point with the value of the critical temperature $T_{crit} = 173$ K and the magnitude of the charge carrier concentration at absolute zero $n_0 = 1.41 \cdot 10^{20} \text{ cm}^{-3}$ (curve 2-1 on Fig.8). Note that in^{8,18} photoluminescence excitation of diamond samples was performed by laser with pulse duration 5-8 ns FWHM.

In^{5,19} the model of a degenerate plasma with the critical values of temperature $T_{crit} = 165$ K and concentration $n_{crit} = 3.33 \cdot 10^{19} \text{ cm}^{-3}$ (curve 1-2 on Fig.8) and the model of a simple liquid near the critical point with the value of the critical temperature $T_{crit} = 160$ K and the amount of the charge carrier concentration at absolute zero $n_0 = 1.0 \cdot 10^{20} \text{ cm}^{-3}$ (curve 2-2 on Fig.8) was also used.

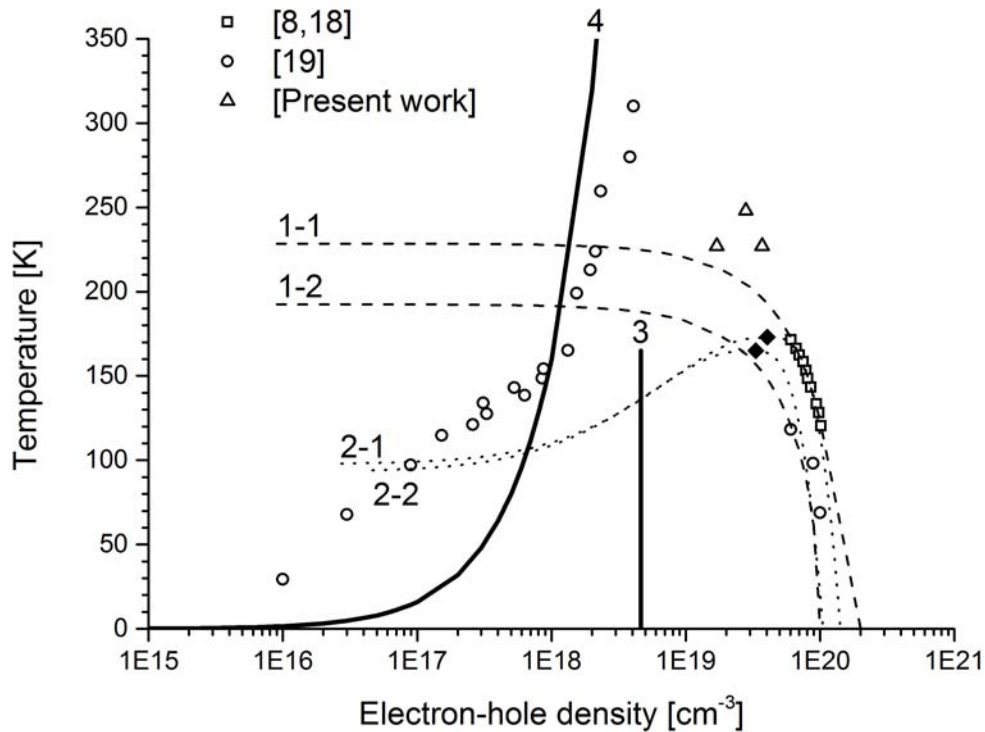


Figure 8. Phase diagram of the electron-hole system in diamond. White squares are experimental data from^{8,18}. White circles are experimental data from¹⁹. 1-1 – degenerate plasma model $T_{crit} = 173$ K, $n_{crit} = 4.05 \cdot 10^{19} \text{ cm}^{-3}$ from¹⁸, 1-2 – degenerate plasma model $T_{crit} = 165$ K, $n_{crit} = 3.33 \cdot 10^{19} \text{ cm}^{-3}$ from¹⁹, 2-1 – liquid-gas transition boundary in Guggenheim model $T_{crit} = 173$ K, $n_0 = 1.41 \cdot 10^{20} \text{ cm}^{-3}$ from¹⁸, 2-2 – liquid-gas transition boundary in Guggenheim model $T_{crit} = 165$ K, $n_0 = 1.0 \cdot 10^{20} \text{ cm}^{-3}$ from¹⁹, 3 - Mott criterion in Thomas-Fermi approximation^{18,19}, 4 – Mott criterion in Debye-Huckel approximation^{18,19}. Black rhombs are two sets of critical temperature and EHP density: $T_{crit} = 160$ и 173 K, $n_{crit} = (3.33 \text{ и } 4.05) \cdot 10^{19} \text{ cm}^{-3}$. White triangles are experimental data of present work.

In¹⁹ authors used laser pulses with sub-picosecond duration (200 fs) for PL excitation. This experimental data (white circles on Fig.8) were obtained not only for the right side of the phase diagram at concentrations higher than the critical, but at concentrations less than the concentration of the Mott transition, which is in the Thomas-Fermi approximation has a threshold (see line 3 on Fig.8), but in the Debye-Huckel approximation increases linearly with the concentration of the EHP (see curve 4 on Fig.8).

Note that the values of the experimental concentration in Fig.8 were obtained by analysis of the form-factors of the spectral components. But the range of values of concentration $4.1 \cdot 10^{18} - 6.0 \cdot 10^{19} \text{ cm}^{-3}$ was not investigated.

Black rhombs in Fig.8 indicate two sets of critical temperature and concentration for condensation EHL. Different values of these variables were defined by the different calculated values in the model of a degenerate plasma and phenomenological model of the gas-liquid transition (see curves 1-1, 1-2, 2-1, 2-2 in Fig.8). As shown in Fig.1, different values of the critical temperature and concentration for condensation EHL were calculated or determined in works^{1,4,8,9}. Furthermore, in the work¹⁸ was claimed that the critical temperature for the condensation EHL is in the range 180-207 K for photoluminescence excitation laser pulses of nanosecond duration. At the same time in work¹², the EHL observed at temperatures less than 120 K during excitation photoluminescence subpicosecond laser pulses. If the critical condensation temperature is determined from the shape of the EHL PL spectra, the critical concentration of the EHL is a calculated parameter.

Significant differences between experimental data of works^{8,18} for nanosecond excitation and experimental data of works^{4,12,19} for femtosecond excitation caused by:

1. Different modes of excitation - quasi-stationary and pulse modes, respectively. In the quasi-stationary mode, the duration of the excitation pulse considerably exceeds the lifetime of the EHL droplets (less than 1 ns), which leads to the nucleation of drops during the excitation pulse. In the pulse mode, the duration of the excitation laser pulse in three orders of magnitude less than the lifetime of the EHL drops, so droplets observed in the PL spectra were formed around the same time.

2. Different peak laser intensities - few to tens of MW/cm² and a few to tens of GW/cm², respectively. The peak intensity of the laser radiation of GW level results in the generation of electron-hole plasma with an initial concentration of more than 10^{20} cm^{-3} , which causes heating of the lattice in the process of thermalization of hot carriers and Auger recombination. This heating leads to a decrease of the critical temperature for the condensation EHL. For example, the authors of¹² had to use too low initial concentrations of EHP 10^{18} cm^{-3} in calculations.

3. Different wavelengths of excitation - 218-220 nm and 215 nm, respectively. Due to the sharp increase in the absorption coefficient of the diamond at the fundamental absorption edge (see Fig.3), photons of smaller energy absorbed in thinner diamond layer. Therefore, the short-wave radiation creates a large initial concentration of the EHP. Moreover, the generation of EHP due to shortwave photons creates "hot" carriers, which transmit more energy to the diamond lattice in thermalization process that reduces the critical temperature.

As can be seen from the phase diagram of Fig.8, the calculated transition of gas FE - EHL in diamond describes the right branch satisfactorily. Whereas, the models used do not give a close description of the experimental curves for the left branch. Noted that, the Mott criterion in Debye-Huckel approximation describes closely the experimental data in the range of EHP concentration of $(1-4) \cdot 10^{18} \text{ cm}^{-3}$. Approximate values of the critical temperature and concentration for the experimental data of this work marked with white triangles on Fig.8.

5. CONCLUSION

In the paper, the integrated PL spectra of two diamond samples, depending on the temperature (80-300 K) and the peak intensity of the laser radiation (7-13 MW/cm²) at wavelengths of 193 nm and 222 nm with 8 ns FWHM duration were studied.

For CVD diamond sample C10 for both excitation wavelengths the FE radiative recombination band was observed in PL spectra at 235.2 nm at all temperatures. The FE band broadened with increasing temperature. For PL excitation at 222 nm with peak radiation intensity of more than 10 MW/cm², the EHL radiative recombination band with a maximum at 239.8 nm was observed in integrated PL spectra. Under the excitation at 193 nm the EHL radiative recombination was not observed clearly.

For HPHT diamond sample C12 for both excitation wavelengths only the FE radiative recombination band was observed in PL spectra at 235.2 nm at all temperatures. The EHL band was not observed clearly.

For CVD sample C10 the dependence of FE intensity on temperature underwent changes with the growth of the peak radiation intensity at 222 nm. At the peak intensity of 7 MW/cm² (insufficient for condensation EHL) this dependence showed a maximum at ~ 150 K. A further increase of the peak radiation intensity leads to the appearance the EHL radiative recombination band in the integrated PL spectrum and displacement of the intensity maximum to 200-210 K due to condensation of FE's in the EHL drops.

For HPHT diamond sample C12 the dependence of FE intensity on temperature showed a maximum at ~ 150 K at all values of the peak radiation intensity at 222 nm.

Analysis of published data on the construction of the phase diagram of gas FE - EHL transition for diamond showed that the existing theoretical concepts of condensation EHL require refinement and further development. In spite of the considerable amount of experimental data, the EHP concentration range of 4.1·10¹⁸ - 6.0·10¹⁹ cm⁻³ and the dependence of the critical temperature for the condensation of the EHL on the initial conditions of the experiment remains unexplored.

REFERENCES

- [1] Vouk, M. A., "Conditions necessary for the formation of the electron-hole liquid in diamond and calculation of its parameters," *J. Phys. C: Solid State Phys.* 12, 2305-2312 (1979).
- [2] Tikhodeev, S. G., "The electron-hole liquid in a semiconductor," *Sov. Phys. Usp.* 28, 1-30 (1985).
- [3] Jeffries, C. D. and Keldysh, L. V. (Eds.), [Electron-Hole Droplets in Semiconductors], North Holland, Amsterdam, 431 (1983).
- [4] Shimano, R., Nagai, M., Horiuchi, K. and Kuwata-Gonokami, M., "Formation of a high Tc electron-hole liquid in diamond," *Phys. Rev. Lett.* 88 (5), 057404 (2002).
- [5] Nagai, M., Shimano, R., Horiuchi, K. and Kuwata-Gonokami, M., "Creation of supercooled exciton gas and transformation to electron-hole droplets in diamond," *Phys. Rev. B* 68, 081202 (2003).
- [6] Keldysh, L.V., in: Ryvkin, S.M. and Shmastsev, V.V. (Eds.), *Proceedings of the Ninth International Conference on the Physics of Semiconductors, Moscow, 1968*, Nauka, Leningrad, 1303 (1968).
- [7] Leys, F.E., March, N.H., Angilella, G.G.N. and Zhang, M.L., "Similarity and contrasts between thermodynamic properties at the critical point of liquid alkali metals and of electron-hole droplets," *Phys. Rev. B* 66, 073314 (2002).
- [8] Sauer, R., Teofilov, N. and Thonke, K., "Exciton condensation in diamond," *Diamond Relat. Mater.* 13 (4-8), 691-699 (2004).
- [9] Lipatov, E.I., Genin, D.E. and Tarasenko, V.F., "The recombination radiation in the synthetic and natural diamond under the action of pulse laser UV radiation," *Russ. Phys. J.* 58 (7), 36-46 (2015).
- [10] Collins, A.T., "Things we still don't know about optical centres in diamond," *Diamond Relat. Mater.* 8, 1455-1462 (1999).
- [11] Takeuchi, D., Watanabe, H., Yamanaka, S., Okushi, H., et al., "Origin of band-A emission in diamond thin films," *Phys. Rev. B* 63, 245328 (2001).
- [12] Naka, N., Omachi, J., Sumiya, H., Tamasaku, K., et al., "Density-dependent exciton kinetics in synthetic diamond crystals," *Phys. Rev. B* 80, 035201 (2009).
- [13] Thonke, K., Schliesing, R., Teofilov, N., Zacharias, H., et al., "Electron-hole drops in synthetic diamond," *Diamond Relat. Mater.* 9, 428-431 (2000).
- [14] Donato, M.G., Messina, G., Verona Rinati, G., Almagro, S., et al., "Exciton condensation in homoepitaxial chemical vapor deposition diamond," *J. Appl. Phys.* 106, 053528 (2009).
- [15] Kozak, M., Trojanek, F., Popelar, T. and Maly, P., "Dynamics of electron-hole liquid condensation in CVD diamond studied by femtosecond pump and probe spectroscopy," *Diamond Relat. Mater.* 34, 13-18 (2013).
- [16] Lipatov, E.I., Lisitsyn, V.M., Oleshko, V.I. and Tarasenko, V.F., "Spectral and kinetic characteristics of the pulsed cathodoluminescence of a natural Iia-type diamond," *Russ. Phys. J.* 50 (1), 52-57 (2007).

- [17] Takiyama, K., Abd-Elrahman, M.I., Fujita, T. and Oda, T., "Photoluminescence and decay kinetics of indirect free excitons in diamonds under the near-resonant laser excitation," *Solid State Commun.* 99 (11), 793-797 (1996).
- [18] Teofilov, N., Schliesing, R., Thonke, K., Zacharias, H., et al., "Optical high excitation of diamond: phase diagram of excitons, electron-hole liquid and electron-hole plasma," *Diamond Relat. Mater.* 12, 636-641 (2003).
- [19] Nagai, M., Shimano, R., Horiuchi, K. and Kuwata-Gonokami, M., "Phase diagram of the quantum degenerate electron-hole system in diamond," *Phys. Status Solidi B* 238 (3), 509-512 (2003).